



Synthesis and characterization of a bis-methanofullerene-4-nitro- α -cyanostilbene dyad as a potential acceptor for high-performance polymer solar cells

Boram Kim^a, Hye Rim Yeom^a, Won-Youl Choi^c, Jin Young Kim^{a,*}, Changduk Yang^{a,b,*}

^a Interdisciplinary School of Green Energy and KIER-UNIST Advanced Center for Energy, Ulsan National Institute of Science and Technology (UNIST), Ulsan 689-798, Republic of Korea

^b Low Dimensional Carbon Materials Center, UNIST, Republic of Korea

^c Department of Metal and Materials Engineering, Gangneung-Wonju National University, Gangneung 210-702, Republic of Korea

ARTICLE INFO

Article history:

Received 20 April 2012

Received in revised form 25 May 2012

Accepted 28 May 2012

Available online 5 June 2012

Keywords:

Methanofullerene

bis-Adduct

bis-PCBM

Dyad

4-Nitro- α -cyanostilbene

ABSTRACT

We report the synthesis, characterization, and electrochemical properties of **bis-PCBM dyad** containing 4-nitro- α -cyanostilbene units for potential usage in efficient organic solar cells. The **bis-PCBM dyad** is fully characterized by NMR, UV–vis absorption, and electrochemical cyclic voltammetry. It is found that the presence of 4-nitro- α -cyanostilbenes affects the cyclic voltammetry and absorption spectrum very little. Whereas the 56 π -electron system in the bis-functionalized fullerene cage significantly influences on the electrochemical and photophysical properties, resulting in up-shifted LUMO and wider absorption compared to PCBM. Although the efficiencies of both conventional and the inverted cells based on P3HT/**bis-PCBM dyad** as the preliminary results are low in comparison with the optimized high-performance PSCs, it is believed that the efficiency would be improved through successful device optimization of P3HT/**bis-PCBM dyad** cells.

© 2012 Elsevier Ltd. All rights reserved.

1. Introduction

A soluble C₆₀ derivative, [6,6]-phenyl-C₆₁ butyric acid methyl ester (PCBM) has affirmed to be an invaluable *n*-type semiconductor for solution-processed organic electronics.^{1–4} Therefore, PCBM has represented the well-studied benchmark acceptor in bulk-heterojunction (BHJ) polymer solar cells (PSCs).^{5–9} Although the modification of the PCBM's structure by changing the substituents aiming at more efficient acceptor materials for PSCs has come into focus, most of the device performance is poorer than or similar to that of PCBM.^{9–13} An important breakthrough was achieved when PCBM was replaced by bis-functionalized 56 π -electron fullerenes^{14–18} ENREF_16, such as bis-PCBM¹⁶ and bis-indene-C₆₀ adducts.^{17,18} These bis-adducts possess higher LUMO energy levels, resulting in higher *V*_{OC} as well as higher power conversion efficiency (PCE) of the P3HT-based PSCs.^{16–18} Another important development was accomplished by the synthesis of [6,6]-phenyl-C₇₁ butyric acid methyl ester (PC₇₁BM) that has a broader absorption in the visible region than PCBM, leading to a positive effect on current generation in PSCs.^{8,19–23}

Despite the enormous advances in the synthesis of fullerene-based dyads and triads to further increase visible absorption,^{24–27} limited success in PSCs has been reported since most of the light-

harvesting organofullerenes suffer from negative side effects, such as insufficient charge transport, inefficient charge-dissociation, or morphology problems.^{12,16} To date, only fullerene-4-nitro- α -cyanostilbene dyad showed superior photovoltaic performance to that of the traditional PCBM.²⁸

In this context, we have designed and synthesized a **bis-PCBM dyad** incorporating 4-nitro- α -cyanostilbene units. Considering possible combined effects from the 56 π -electron system by the bis-adduct framework and the increased light absorption in the visible region by the additional chromophores, the **bis-PCBM dyad** is rationally expected to display excellent performance and its structural motif is outlined in Fig. 1.

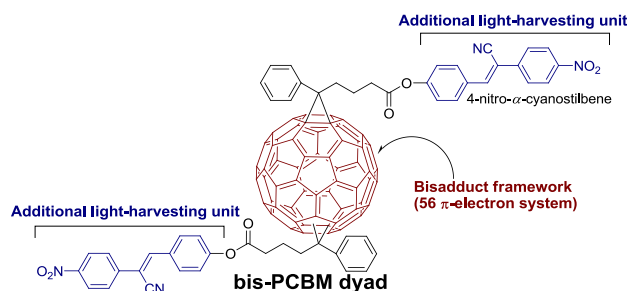
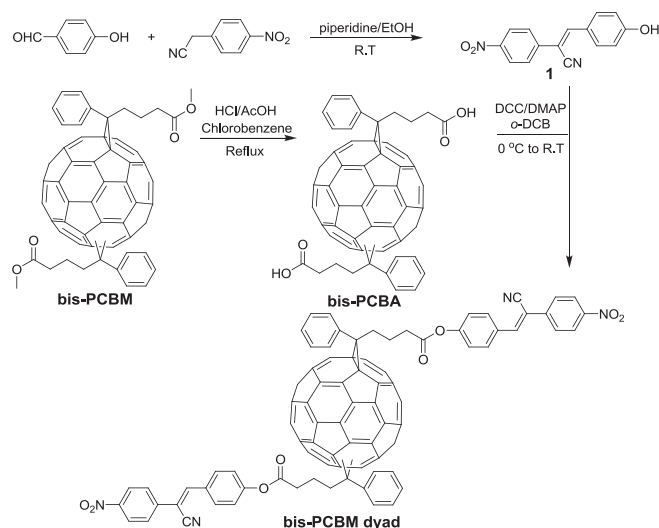


Fig. 1. Rational design motif of **bis-PCBM dyad**; 4-nitro- α -cyanostilbene was chosen as additional light-harvesting unit to provide a higher *J*_{sc}. In principle, the LUMO can be raised by bis-adduct framework due to 56 π -electron system.

* Corresponding authors. Interdisciplinary School of Green Energy and KIER-UNIST Advanced Center for Energy, Ulsan National Institute of Science and Technology (UNIST), Ulsan 689-798, Republic of Korea; e-mail addresses: jykim@unist.ac.kr (J.Y. Kim), yang@unist.ac.kr (C. Yang).

2. Results and discussion

The synthesis of the intermediates and **bis-PCBM dyad** is shown in Scheme 1. Previously, Sharma and co-workers prepared the 4-nitro-4-hydroxy- α -cyanostilbene as a dark green solid *via* Knoevenagel condensation between 4-hydroxybenzaldehyde and 4-nitrobenzylcyanide in ethanol in the presence of sodium hydroxide.²⁹ Later, aiming at improving the PSCs, they reported the synthesis and evaluation of a 4-nitro- α -cyanostilbene-based PCBM, which, given its high device performance, identified a new effective modification strategy for fullerenes in PSCs.²⁸



Scheme 1. Synthetic route to **bis-PCBM dyad**.

However, our initial attempt to synthesize 4-nitro-4-hydroxy- α -cyanostilbene by the procedure described in the literature above, gave, by the inspection of the ^1H NMR spectrum, inseparable complex mixtures. Despite the utilization of various purification tools, the pure greenish product could not be isolated. A characteristic solubility of the mixtures in water was a main problem of the product separation. This is probably due to the formation of salt sodium phenoxides since sodium hydroxide is strong enough base to react with 4-hydroxybenzaldehyde as acidic phenolic compound. We then proceeded to investigate the synthesis of 4-nitro-4-hydroxy- α -cyanostilbene (**1**) through the Knoevenagel reaction catalyzed by piperidine in ethanol, successfully affording a pure 'red' product in quantitative yield, an observation at odds with the color reported by Sharma et al. (see the digital photograph and ^1H NMR in Fig. 2a as well as ^{13}C NMR in the SI for further information).

As well, bis-PCBM was obtained as a by-product of the preparation of PCBM.^{1,16} After isolating the unreacted C_{60} and PCBM by column chromatography in the regular manner, the isomeric bis-PCBMs were collected upon elution with dichloromethane. And then, the esters were hydrolyzed with hydrochloric acid/acetic acid to the corresponding dicarboxylic acid-functionalized bis-PCBA. The acid bis-PCBA was found to be insoluble in most organic solvents, most likely due to the combination of intermolecular hydrogen bonding and C_{60} – C_{60} interactions.¹ Finally, **bis-PCBM dyad** was prepared by a Steglich esterification (DCC/DMAP)^{30,31} of **1** with bis-PCBA. The structure of **bis-PCBM dyad** was fully identified by ^1H and ^{13}C NMR (Fig. 2b and c). Owing to two large substituents, the target product is easily soluble in chloroform, tetrahydrofuran (THF), chlorobenzene (CB) and *ortho*-dichlorobenzene (*o*-DCB). In contrast to the color previously described for 4-nitro- α -cyanostilbene-PCBM (dark green), the obtained product **bis-PCBM dyad**

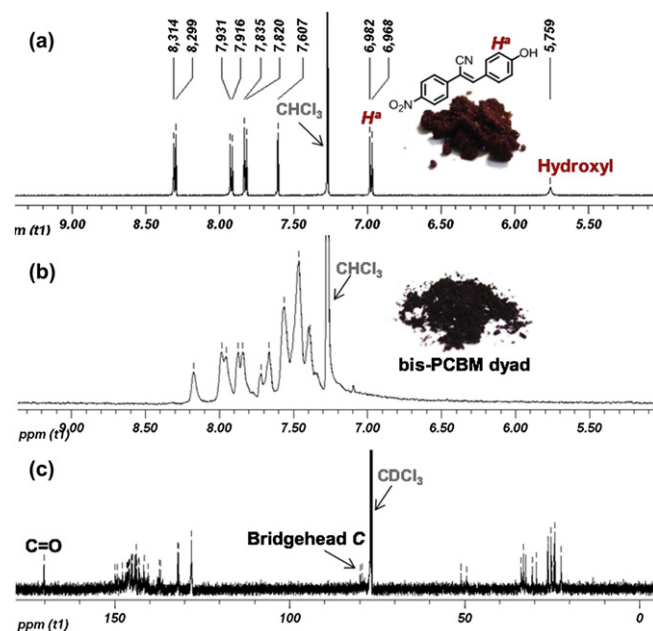


Fig. 2. ^1H NMR (a) of **1** and ^1H & ^{13}C NMR (b, c) spectra of **bis-PCBM dyad** in CDCl_3 . The digital photographs of **1** and **bis-PCBM dyad**.

turned out to be a dark red solid (see the digital photograph in Fig. 2b). In the ^1H NMR spectrum, as a result of the successful ester formation, we can clearly see a disappearance of the δ_{OH} resonances at 5.75 ppm as well as an apparent up-field shift of the peaks ($\delta=6.98$ ppm) denoting the aromatic signals *ortho* to the phenolic benzene ring unit in 4-nitro-4-hydroxy- α -cyanostilbene. The ^{13}C NMR spectroscopy shows a resonance in the carbonyl region at $\delta=170.22$ ppm and a lot of carbon signals in the sp^2 region ($\delta=127$ – 150 ppm). Additionally, the spectrum displays two single intensity resonances assigned to sp^3 -hybridized bridgehead carbon atoms at $\delta=79.83$ ppm and 79.25 ppm as well as signals at around 50 ppm corresponding to the quaternary carbon atoms of the fullerene unit, in accordance with a [6,6]-closed methanofullerene. The remaining signals are attributable to the carbon atoms of the butyl chains in PCBM.

Fig. 3 depicts the UV–vis absorption characteristics of 4-nitro-4-hydroxy- α -cyanostilbene (**1**), PCBM, bis-PCBM, and **bis-PCBM dyad** in chloroform solution. PCBM shows strong absorption at 330 nm whereas the absorption maximum of **1** is at 365 nm. The absorption of **bis-PCBM dyad** is non-superimposable on the sum of the absorption spectra of **1** and bis-PCBM (see bis-PCBM in Fig. 3 as well),

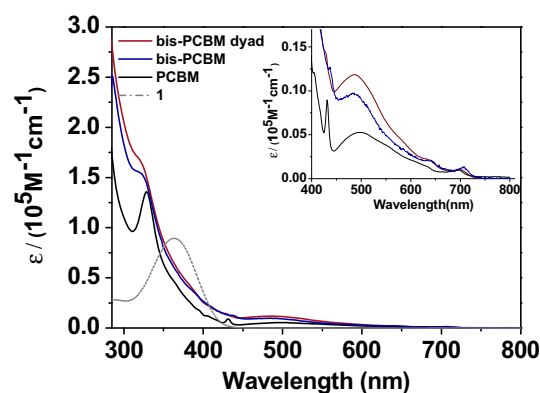


Fig. 3. UV–Vis absorption of **1**, PCBM, bis-PCBM, and **bis-PCBM dyad** in CHCl_3 solution.

implying an evidence of the electronic interaction of the two chromophores.^{32,33} Interestingly, the spectrum of **bis-PCBM dyad** displays an increased and wider absorption compared to PCBM, with a shoulder peak at ca. 430 nm as characteristic of [6,6]-closed ring isomer. The relatively higher absorption of **bis-PCBM dyad** in the visible region can be attributed, in part, to a highly broken symmetry of the fullerene core, leading to the lowest-energy transitions being formally dipole allowed.^{34,35} A closer view of the two spectra (PCBM and **bis-PCBM dyad**) discloses, furthermore, a red-shifted band at ~ 707 nm relative to the PCBM (697 nm). From the herein observed spectral features, it is safe to assume that **bis-PCBM dyad** would be able to absorb more solar energy and contribute to an improved performance.

The electrochemical properties of **bis-PCBM dyad** were studied by cyclic voltammetry (CV), where PCBM data obtained in this study for comparison is also shown in Fig. 4. In *o*-ODCB, each compound exhibits three well-defined, single-electron, quasireversible waves, which is in sharp contrast with the results reported for 4-nitro- α -cyanostilbene-PCBM with only one reduction peak.²⁸ The half-cell potentials (defined as $E_1 = 0.5(E_{p,c} + E_{p,a})$) for the reduction of the PCBM and **bis-PCBM dyad** relative to Fc/Fc⁺ are -1164 , -1540 , -2036 mV, and -1261 , -1587 , -2260 mV, respectively. The **bis-PCBM dyad** lifts its LUMO level by ~ 100 meV, from -3.636 eV (PCBM) to -3.539 eV, because of the extraction of two more π -electrons from the fullerene core. This reveals an obvious similarity to the difference between LUMO levels of PCBM and bis-PCBM.¹⁶ We do not observe an additional up-shift of the LUMO because of the inductive effect of the strong electron withdrawing nitro and cyano groups in the **bis-PCBM dyad** on the redox behavior, as opposed to the report by Sharma et al.²⁸ The fully optimization of the PSC device based on P3HT/**bis-PCBM dyad** is an extraordinarily time-consuming process since a complex region isomeric mixture of the bis-adduct has any negative side effects on the charge-transport properties.¹⁶

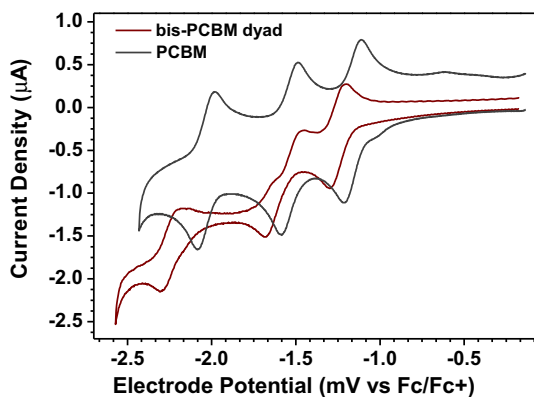


Fig. 4. Cyclic voltammograms of PCBM and **bis-PCBM dyad** in *o*-DCB solution. Experimental conditions: values for $0.5(E_{pa} + E_{pc})$ in V versus Fc/Fc⁺; 10^{-4} – 10^{-3} mol/L *o*-DCB solution; Bu₄NClO₄ (0.1 M) as supporting electrolyte; Pt wire as counter electrode; 50 mV/s scan rate.

To demonstrate potential applications of the **bis-PCBM dyad** in PSCs, we used P3HT as an electron donor and **bis-PCBM dyad** as an electron acceptor. The blends were spin-coated from a mixture of solvents (chloroform/5% acetone) containing the P3HT/**bis-PCBM dyad** and subsequent thermal annealing 120 °C. The device architectures of the conventional and the inverted devices are ITO/PEDOT:PSS/P3HT:**bis-PCBM dyad** (1:1 w/w)/Al and ITO/TiO_x/P3HT:**bis-PCBM dyad** (1:1 w/w)/MoO₃/Au, respectively. In the inverted devices, MoO₃ as the hole transport layer and TiO_x as the electron transport layer were deposited. The device structures of the regular and inverted polymer solar cells are shown in Fig. 5a and b. All data were obtained under white light AM 1.5G

illumination from a calibrated solar simulator with irradiation intensity of 100 mW/cm². The device performance of a solar cell is determined by the open-circuit voltage (V_{OC}), short-circuit current (J_{SC}), and fill factor (FF). The power conversion efficiency (η_e) of a solar cell is given as $\eta_e = (J_{SC} \cdot V_{OC} \cdot FF) \cdot 100 / P_{INC}$, where P_{INC} is the intensity of incident light. Higher values of those three parameters yield larger light-to-electricity power conversion efficiency.

The PCE up to 0.76% is observed for the conventional P3HT:**bis-PCBM dyad** solar cells with a V_{OC} of 0.69 V, a short circuit current density (J_{SC}) of 3.05 mA/cm², and a fill factor (FF) of 36%. On the other hand, under the same white light illumination, the P3HT:**bis-PCBM dyad**-based inverted cells exhibit a J_{SC} of 1.06 mA/cm², a V_{OC} of 0.47 V, and a FF of 31%. It yields a substantially lower PCE of 0.16% because of its decreased photocurrent. Work is in progress in order to find optimal conditions for the PSCs based on P3HT/**bis-PCBM dyad**.

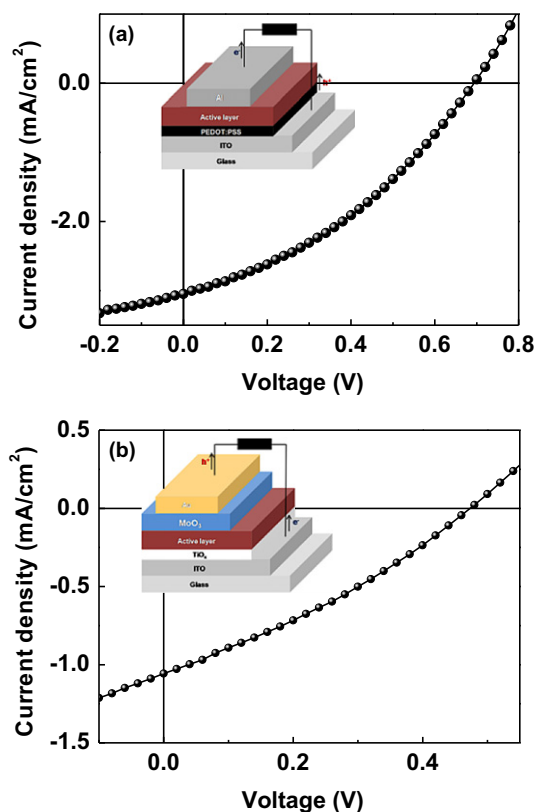


Fig. 5. J - V characteristics of conventional (a) and the inverted (b) devices under AM 1.5G illumination from a calibrated solar simulator with an intensity of 100 mW/cm². Inset is a schematic of the device architectures, respectively.

3. Conclusion

Aspiring to improve efficiency of the PSCs, we have presented a novel type of fullerene, **bis-PCBM dyad** bearing 4-nitro- α -cyanostilbene moieties, clearly identified through a combination of ¹H and ¹³C NMR spectra. From the electrochemical and photophysical properties of the **bis-PCBM dyad**, one can conclude that the 4-nitro- α -cyanostilbene chromophores influence the absorption and electronic energy levels of the C₆₀ derivatives very little. By virtue of 56 π -electron system in fullerene framework, the **bis-PCBM dyad** has a higher LUMO level and stronger absorption than PCBM, which should potentially be a highly helpful for minimizing the energy loss in the electron transfer from the donor to the acceptor material as well as increasing current generation in BHJ solar cells. By optimizing the device fabrication process, the photovoltaic

performance of **bis-PCBM dyad** as acceptor blended with P3HT would be significantly superior to that of the traditional PCBM. As initial results, the efficiency obtained from the conventional structure device is 0.76%, while the PCE of the inverted device reaches 0.16%. Through successful device optimization of P3HT/**bis-PCBM dyad** cells, the high efficiency would be expected in the near future.

Thus, future efforts will focus on testing the influence of **bis-PCBM dyad** in combination with P3HT on the performance of PSCs.

4. Experimental section

4.1. Materials and instruments

All starting materials were purchased either from Aldrich or Acros and used without further purification. All solvents are ACS grade unless otherwise noted. Anhydrous THF was obtained by distillation from sodium/benzophenone prior to use. Anhydrous toluene was used as received. ^1H NMR and ^{13}C NMR spectra were recorded on a Varian VNMRS 600 spectrophotometer and MALDI-MS spectra were obtained from Ultraflex III (Bruker, Germany). UV–vis spectra were taken on Cary 5000 (Varian USA) spectrophotometer. Cyclic voltammetry (CV) measurements were performed on AMETEK VersaSTAT 3 with a three-electrode cell in a nitrogen 0.1 M tetrabutylammonium perchlorate solution in *o*-DCB at a scan rate of 50 mV/s at room temperature. Ag used as the Ag/Ag⁺ (0.1 M of AgNO₃ in acetonitrile) reference electrode, platinum counter electrode, and polymer coated platinum working electrode, respectively. The Ag/Ag⁺ reference electrode was calibrated using a ferrocene/ferrocenium redox couple as an internal standard, whose oxidation potential is set at -4.8 eV with respect to zero vacuum level. The LUMO levels of polymers were obtained from the equation $\text{LUMO} = -(E_{\text{Red}}^{\text{onset}} - E_{\text{(ferrocene)}}^{\text{onset}}) + 4.8$ eV. $E_{\text{g}}^{\text{opt}} = 1240/\lambda_{\text{edge}}$. $\text{HOMO} = -(E_{\text{g}}^{\text{opt}} - \text{LUMO})$.

4.2. Fabrication of conventional and inverted photovoltaic cells

Two-type photovoltaic cells were fabricated on ITO-coated glass substrates. The ITO-coated glass substrates were first cleaned with detergent, ultrasonicated in water, acetone and isopropyl alcohol, and dried overnight in an oven. In conventional cells, PEDOT:PSS (AI 4083) was spin-cast on cleaned ITO substrates after a UV–ozone treatment for 15 min and heated at 140 °C for 10 min in air. Subsequently, the active layer was coated in a glove box. The solution containing a mixture of P3HT:**bis-PCBM dyad** (1:1 w/w) in a mixture of solvents (chloroform/5% acetone) with a concentration of 11 mg/mL and P3HT:**bis-PCBM dyad** (1:1) in a mixture of solvents (chloroform/5% acetone) with a concentration of 13 g/mL was spin-cast on top of PEDOT:PSS film. After then, the top electrode (Al) was deposited on the active layer in a vacuum ($<10^{-6}$ Torr) thermal evaporator. Inverted solar cells were fabricated on ITO-coated glass substrates. A TiO_x precursor solution was prepared using the sol-gel method. The TiO_x precursor solution was spin-cast on cleaned ITO substrates after a UV–ozone treatment for 15 min and heated at 80 °C for 10 min in air for conversion to TiO_x by hydrolysis. Subsequently, the TiO_x-coated substrates were transferred into a glove box. A solution containing a mixture of P3HT:**bis-PCBM dyad** (1:1 w/w) in a mixture of solvents (chloroform/5% acetone) was spin-cast on top of TiO_x films. Then, a thin layer of MoO₃ film (≈ 5 nm) was evaporated on top of the active layer. Finally, the anode (Au, ≈ 95 nm) was deposited on the active layer in a vacuum ($<10^{-6}$ Torr) thermal evaporator. The cross-sectional area of each of the electrode defines the active area of the device as 13.5 mm². Photovoltaic cell measurements were carried out inside the glove box using a high quality optical fiber to guide the light from the solar simulator equipped with a Keithley 2635A source measurement

unit. The J – V curves for the devices were measured under AM 1.5G illumination at 100 mA/cm².

4.3. Synthesis of 4-nitro-4-hydroxy- α -cyanostilbene (1)

To a mixture of the 4-hydroxybenzaldehyde (2.0 g, 16.39 mmol) and 4-nitrobenzylcyanide (2.66 g, 16.39 mmol) in absolute EtOH (40 mL), was added with piperidine (2.43 mL, 24.58 mmol) portionwise, stirred at room temperature for 3 h, cooled to 0 °C, and filtered. The precipitate was washed with EtOH, dried to yield **1** (95%). ^1H NMR (600 MHz, CDCl₃): δ (ppm) 8.30 (d, $J=9$ Hz, 2H), 7.92 (d, $J=8.4$ Hz, 2H), 7.82 (d, $J=9$ Hz, 2H), 7.60 (s, 1H), 6.98 (d, $J=8.4$ Hz, 2H), 5.75 (s, 1H). ^{13}C NMR (150 MHz, acetone-*d*₆): δ (ppm) 161.50, 147.37, 145.81, 141.52, 132.32, 126.36, 124.75, 123.92, 117.79. Elemental analysis: C, 67.67; H, 3.79; N, 10.52; O, 18.03; Found: C, 67.90; H, 3.89; N, 10.78; O, 18.15. Mp 204 °C. FTIR (ν/cm^{-1}): 3417, 2171, 1585, 1525, 1322.

4.4. Synthesis of bis-[6,6]-phenyl C₆₁-butyric acid (bis-PCBA)

To a solution containing bis-PCBM (1.0 g, 0.90 mmol) in chlorobenzene was added acetic acid (70 mL) and concentrated hydrochloric acid (20 mL). The mixture was heated to reflux overnight. The solvent was removed *in vacuo* and the precipitate was collected by filtration. The course of the reaction was followed by TLC (after complete conversion, R_f is 0.0) The crude product was washed with methanol and a solvent mixture of MeOH:diethyl ether (1:1 v/v) several times to give quantitative yield. Mp 302 °C. FTIR (ν/cm^{-1}): 1711, 1438, 1421, 1210, 1190, 1157, 734, 573, 511.

4.5. Synthesis of bis-PCBM dyad

Compound **1** (0.18 g, 0.69 mmol) was mixed with bis-PCBA (0.17 g, 0.15 mmol) and 4-*N,N*-dimethylaminopyridine (DMAP) (0.4 g, 3.40 mmol) in *o*-DCB (60 mL). This mixture was treated in an ultrasonicator bath for 10 min, then cooled down to 0 °C in an ice/water bath. Finally, *N,N'*-dicyclohexylcarbodiimide (DCC) (1.58 g, 7.65 mmol) was added to the mixture quickly with a syringe. The mixture was stirred at 0 °C for 5 h and then warmed up to room temperature with continuously stirring for 3 d. The mixture was concentrated to ca. 3 mL using a rotary evaporator, followed by addition of excess MeOH. The solid was separated by centrifugation (3000 rpm/30 min), washed with MeOH twice and then with diethyl ether twice, and further purified by column chromatography on silica gel with dichloromethane as eluent to yield **bis-PCBM dyad** (75% as a dark red solid). ^1H NMR (600 MHz, CDCl₃): δ (ppm) 8.20–8.15 (m, 4H), 7.99–7.91 (m, 4H), 7.87–7.81 (m, 4H), 7.75–7.61 (m, 4H), 7.52–7.21 (m, 12H). ^{13}C NMR (150 MHz, CDCl₃): δ (ppm) 170.22, 149.94, 149.81, 149.21, 147.81, 146.75, 146.61, 146.45, 146.43, 146.40, 164.20, 146.12, 146.08, 146.00, 145.92, 145.84, 145.77, 145.39, 145.34, 145.23, 145.12, 144.99, 144.29, 144.23, 144.07, 144.04, 143.88, 143.74, 143.16, 143.09, 142.81, 141.66, 141.50, 140.47, 140.26, 137.70, 137.56, 137.31, 136.89, 132.13, 131.90, 131.77, 128.30, 128.15, 128.02, 127.88, 127.85, 79.83, 79.25, 51.05, 51.00, 50.96, 49.48, 49.38, 33.92, 33.83, 33.77, 33.64, 33.18, 33.06, 32.60, 32.57, 30.78, 30.71, 30.64, 29.48, 26.28, 26.22, 25.30, 25.09, 24.54, 24.31, 22.52, 22.47, 22.41. Elemental Analysis: C, 85.71; H, 2.57; N, 3.57; O, 8.15; Found: C, 85.37; H, 2.34; N, 3.47; O, 8.12. MALDI-TOF-MS m/z : $[\text{M}]^+ = 1569$. Mp 242 °C. FTIR (ν/cm^{-1}): 2195, 1705, 1575, 1543, 1517, 1443, 1431, 1335, 1312, 1233, 1201, 1149, 701, 521.

Acknowledgements

This work was supported by Basic Science Research Program through the National Research Foundation of Korea (NRF) funded by the Ministry of Education, Science and Technology (2010-

0002494) and the National Research Foundation of Korea Grant funded by the Korean Government (MEST) (2010-0019408), (2010-0026163), (2010-0026916) (NRF-2009-C1AAA001-0093020).

Supplementary data

^1H and ^{13}C NMR spectra of **1**. Supplementary data related to this article can be found online at <http://dx.doi.org/10.1016/j.tet.2012.05.114>.

References and notes

- Hummelen, J. C.; Knight, B. W.; Lepeq, F.; Wudl, F.; Yao, J.; Wilkins, C. L. *J. Org. Chem.* **1995**, *60*, 532–538.
- Janssen, R. A. J.; Christiaans, M. P. T.; Pakbaz, K.; Moses, D.; Hummelen, J. C.; Sariciftci, N. S. *J. Chem. Phys.* **1995**, *102*, 2628–2635.
- Sariciftci, N. S.; Smilowitz, L.; Heeger, A. J.; Wudl, F. *Science* **1992**, *258*, 1474–1476.
- Yu, G.; Gao, J.; Hummelen, J. C.; Wudl, F.; Heeger, A. J. *Science* **1995**, *270*, 1789–1791.
- Li, G.; Shrotriya, V.; Huang, J. S.; Yao, Y.; Moriarty, T.; Emery, K.; Yang, Y. *Nat. Mater.* **2005**, *4*, 864–868.
- Ma, W. L.; Yang, C. Y.; Gong, X.; Lee, K.; Heeger, A. J. *Adv. Funct. Mater.* **2005**, *15*, 1617–1622.
- Padinger, F.; Rittberger, R. S.; Sariciftci, N. S. *Adv. Funct. Mater.* **2003**, *13*, 85–88.
- Cheedarala, R. K.; Kim, G. H.; Cho, S.; Lee, J.; Kim, J.; Song, H. K.; Kim, J. Y.; Yang, C. J. *Mater. Chem.* **2011**, *21*, 843–850.
- Yang, C.; Kim, J. Y.; Cho, S.; Lee, J. K.; Heeger, A. J.; Wudl, F. *J. Am. Chem. Soc.* **2008**, *130*, 6444–6450.
- Choi, J. H.; Son, K. I.; Kim, T.; Kim, K.; Ohkubo, K.; Fukuzumi, S. *J. Mater. Chem.* **2010**, *20*, 475–482.
- Troshin, P. A.; Hoppe, H.; Renz, J.; Egginger, M.; Mayorova, J. Y.; Goryochev, A. E.; Peregudov, A. S.; Lyubovskaya, R. N.; Gobsch, G.; Sariciftci, N. S.; Razumov, V. F. *Adv. Funct. Mater.* **2009**, *19*, 779–788.
- Zhao, G. J.; He, Y. J.; Xu, Z.; Hou, J. H.; Zhang, M. J.; Min, J.; Chen, H. Y.; Ye, M. F.; Hong, Z. R.; Yang, Y.; Li, Y. F. *Adv. Funct. Mater.* **2010**, *20*, 1480–1487.
- Kim, J.; Yun, M. H.; Lee, J.; Kim, J. Y.; Wudl, F.; Yang, C. *Chem. Commun.* **2011**, 3078–3080.
- Kang, H.; Cho, C. H.; Cho, H. H.; Kang, T. E.; Kim, H. J.; Kim, K. H.; Yoon, S. C.; Kim, B. J. *ACS Appl. Mater. Interfaces* **2012**, *4*, 110–116.
- Kim, K. H.; Kang, H.; Nam, S. Y.; Jung, J.; Kim, P. S.; Cho, C. H.; Lee, C.; Yoon, S. C.; Kim, B. J. *Chem. Mater.* **2011**, *23*, 5090–5095.
- Lenes, M.; Wetzelaer, G.; Kooistra, F. B.; Veenstra, S. C.; Hummelen, J. C.; Blom, P. W. M. *Adv. Mater.* **2008**, *20*, 2116–2119.
- He, Y. J.; Chen, H. Y.; Hou, J. H.; Li, Y. F. *J. Am. Chem. Soc.* **2010**, *132*, 1377–1382.
- Zhao, G. J.; He, Y. J.; Li, Y. F. *Adv. Mater.* **2010**, *22*, 4355–4358.
- Wienk, M. M.; Kroon, J. M.; Verhees, W. J. H.; Knol, J.; Hummelen, J. C.; van Hal, P. A.; Janssen, R. A. J. *Angew. Chem., Int. Ed.* **2003**, *42*, 3371–3375.
- Yun, M. H.; Kim, G. H.; Yang, C.; Kim, J. Y. *J. Mater. Chem.* **2010**, *20*, 7710–7714.
- Kim, G.; Yeom, H. R.; Cho, S.; Seo, J. H.; Kim, J. Y.; Yang, C. *Macromolecules* **2012**, *45*, 1847–1857.
- Lee, J.; Yun, M. H.; Kim, J.; Kim, J. Y.; Yang, C. *Macromol. Rapid Commun.* **2012**, *33*, 140–145.
- Kim, J.; Yun, M. H.; Anant, P.; Cho, S.; Jacob, J.; Kim, J. Y.; Yang, C. *Chem.—Eur. J.* **2011**, *17*, 14681–14688.
- Gómez, R.; Segura, J. L.; Martín, N. *Org. Lett.* **2005**, *7*, 717–720.
- Segura, J. L.; Gómez, R.; Martín, N.; Luo, C. P.; Guldi, D. M. *Chem. Commun.* **2000**, 701–702.
- Segura, J. L.; Martín, N. *Tetrahedron Lett.* **1999**, *40*, 3239–3242.
- Martín, N.; Sánchez, L.; Illescas, B.; Pérez, I. *Chem. Rev.* **1998**, *98*, 2527–2547.
- Mikroyannidis, J. A.; Kabanakis, A. N.; Sharma, S. S.; Sharma, G. D. *Adv. Funct. Mater.* **2011**, *21*, 746–755.
- Mikroyannidis, J. A.; Tsagkourinos, D. V.; Balraju, P.; Sharma, G. D. *Org. Electron.* **2010**, *11*, 1242–1249.
- Wang, M. F.; Heeger, A. J.; Wudl, F. *Small* **2011**, *7*, 298–301.
- Neises, B.; Steglich, W. *Angew. Chem., Int. Ed. Engl.* **1978**, *17*, 522–524.
- Liu, Y.; Zhao, J. *Chem. Commun.* **2012**, 3751–3753.
- Brites, M. J.; Santos, C.; Nascimento, S.; Gigante, B.; Luftmann, H.; Fedorov, A.; Berberan-Santos, M. N. *New J. Chem.* **2006**, *30*, 1036–1045.
- Kordatos, K.; Da Rosa, T.; Prato, M.; Bensasson, R. V.; Leach, S. *Chem. Phys.* **2003**, *293*, 263–280.
- Meng, X.; Zhang, W.; Tan, Z.; Li, Y. F.; Ma, Y.; Wang, T.; Jiang, L.; Shu, C.; Wang, C. *Adv. Funct. Mater.* **2012**, *22*, 2187–2193.